Stability Problems of Pyramidal von Mises Planar Trusses with Geometrical Imperfection

MARTIN KALINA[1a]
[1]Institute of Structural Mechanics
[1]Brno University of Technology
[1]Faculty of Civil Engineering, Veveří Str. 95, 602 00, Brno
[1]CZECH REPUBLIC
[1a]kalina.m1@fce.vutbr.cz http://www.vutfu.cz/

Abstract: - The present paper deals with an analysis of pyramidal von Mises planar trusses with or without initial geometric imperfection. Models with real geometrical and material parameters were applied. The models had the cross section of a hot-rolled steel profile. The paper describes a dynamic relaxation method which monitors the potential energy of the von Mises planar truss loaded by displacement of top hinge. The transformed potential energy was depicted in flat and three-dimensional maps. Static eqilibrium paths and positions of chosen bifurcation points were found.

Key-Words: - Pyramidal von Mises planar truss, Nonlinear system, Dynamical relaxation method, Potential energy, Static eqilibrium paths, Bifurcation point

1 Introduction

Stability is the capacity of a structural element or a system to resist to forces disturbing its equilibrium position [1]. The stability loss means a structure collapse, which can occur due to a very small displacement. The small displacement can be a random imperfection which is, in the structure element, due to production or assembly [2-4]. The stability and initial imperfections are key phenomena influencing the reliability of slender thin-walled plate girders [5-8] and bar structures [9], [10].

There exist numerous studies examining the influence of imperfections on the stability of bar structures loaded by static loading, see, e.g., [11], [12]. Many of safety critical objects are assessed by applying the methods of reliability theory or probabilistic risk assessment [13-16]. The in-stability of static equilibrium of the structure in relation to initial imperfections is generally a negative phenomenon which can be studied by the sensitivity analysis [17-20]. The majority of reliability studies of common building structures are aimed at limit states, and form an important subset of decision-making problems based on multiple criteria [21-23].

Optimization problems of real slender structures are usually solved on behalf of geometrically and material nonlinear solutions by the finite element method [24-26]. Theoretical possibilities of modern geometrically nonlinear algorithms are, however, much larger than those generally applied to engineering approaches. The application of usual geometrically nonlinear methods to analyse the deformations of real structures gives the deformations which are relatively small in comparison with lengths of bars of frame systems. The challenge of basic research became the stability problems of elastic pyramidal von Mises planar trusses with large displacements [27]. A large range of stability problems can be studied on behalf of algorithms of modern nonlinear mechanics [28].

The von Mises planar truss is a bar structure consisting of two bars connected with one another in the top hinge [29], [30]. The study of von Mises planar truss is important for understanding the stability problems of these bar structures. The aim of the presented study, which follows work published in [32], is an analysis of stability loss of high von Mises planar trusses with initial imperfections. The stability analysis is solved, applying the geometrically nonlinear solution. The conditions of static equilibrium of the nonlinear system are calculated by means of the so-called dynamic method which searches for the deformations of von Mises planar truss in dependence on forced displacement of top hinge in the coordinate grid. The monitoring of potential energy of the top hinge makes it possible to find the stable static eqilibrium state, the unstable static eqilibrium state and their mutual transition between each other (bifurcation point) of the von Mises planar truss. The maps of transformed potential energies were applied to clearly illustrate the values of potential energies.

2 Model and method used

Fig.1 presents the model of the von Mises planar truss divided in hinges and assembled of segments transferring the normal stiffness of translational spring, and the bending stiffness of rotational spring, see [32].

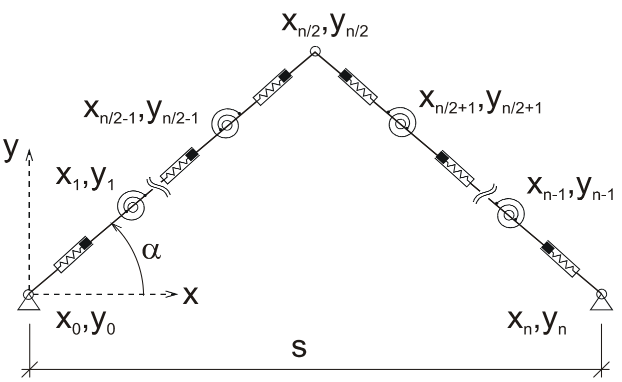

Fig.1 Von Mises planar truss

The internal force F_l in the translation spring, and the internal moment M_φ in the rotational spring will be calculated as:

$$F_l = k_l \cdot d_l,\ M_\varphi = k_\varphi \cdot d_\varphi, \tag{1}$$

where k_l is the stiffness of translational spring, d_l is the elongation of translational spring, k_φ is the stiffness of rotational spring, and d_φ is the angular displacement of rotational spring. The potential energy U, accumulated between the translational and the rotational springs, will be, for the von Mises planar truss, subsequently written as:

$$U = \frac{1}{2}\left(k_l \sum_{i=1}^{n_l} d_{li}^2 + k_\varphi \sum_{i=1}^{n_\varphi} d_{\varphi i}^2\right), \tag{2}$$

where n_l is the number of translational springs, and n_φ is the number of rotational springs. The deformation state of the described von Mises planar truss is accurately given by the position of each hinge. This position of hinge is determined by the coordinate (x_i, y_i), where i denotes the hinge index. The following equation will be used to calculate the elongation of translational spring:

$$d_{li} = l_i - l,\ l_i = \sqrt{(x_{i+1} - x_i)^2 + (y_{i+1} - y_i)^2}, \tag{3}$$

where l is original length of the segment, l_i is the length of the segment after displacement. To calculate the angular displacement of rotational springs, the equation will be specified:

$$d_{\varphi i} = \varphi_{i+1} - \varphi_i,\ \tan\varphi_i = \frac{y_{i+1} - y_i}{x_{i+1} - x_i}, \tag{4}$$

where φ_i is the angular displacement of segment i (the segment between hinges i and i+1). The curvature of the left bar represents the initial geometrical imperfection (bow imperfection). This geometrical imperfection was considered here in form of one half wave of the function sinus.

$$w(x) = a \cdot \sin\left(\frac{\pi x}{L}\right), \tag{5}$$

where a is the amplitude of one half-wave of function sinus, L is the bar length. Including this imperfection into the lengths of segments, and of angles of rotational springs, the bar will be modified (bent) still in the initial state, so that the final shape of von Mises planar truss will have zero stress.

The model is formulated as a nonlinear dynamic system. Static eqilibrium paths of the model are found by dynamical relaxation thanks to the linear viscous damping force acting on the hinges. The mass of the bar is concentrated in hinges. Due to this assumption, the dynamic equations can be derived, applying the Newton principle, in the following equation:

$$\begin{aligned} \frac{\mathrm{d}x_i}{\mathrm{d}t} &= v_{xi}, \frac{\mathrm{d}v_{xi}}{\mathrm{d}t} = \frac{1}{m}\left(R_{xi} - c v_{xi}\right), \\ \frac{\mathrm{d}y_i}{\mathrm{d}t} &= v_{yi}, \frac{\mathrm{d}v_{yi}}{\mathrm{d}t} = \frac{1}{m}\left(R_{yi} - c v_{yi}\right), \end{aligned} \tag{6}$$

where c is the damping coefficient, m is the mass of the hinges, v_{xi} and v_{yi} are the velocity vector components of the hinges, and R_{xi} and R_{yi} are the vector components of the resultant force R_i by which the springs act on the hinge. This system is solved by the Symplectic Euler method [31], which was generated by rearrangement of the explicite Euler method.

3 Mapping of potential energy

The model of the von Mises planar truss is loaded by the controlled displacement in point $x_{n/2}$, $y_{n/2}$ (further on, only top hinge) [32]. At each displacement of top hinge, the von Mises planar truss relaxes for a certain time. After this time, the potential energy of the top hinge is recorded.

The controlled displacement takes place from coordinate x from the value of half of span $s/2$ in horizontal direction along the coordinate x, until the coordinate x of top hinge reaches the value of the bar length. Vertical displacement of the hinge is mapped within the $<s/2;\ L>$. In the step when x=L, the vertical displacement of top hinge takes place opposite to the direction of coordinate y, and the top hinge starts displacing back to the original coordinate x, recorded within the interval $<L;\ s/2>$. In the step, when $x = s/2$, the vertical displacement of the top hinge takes place again opposite to the direction of coordinate y, and the top hinge starts displacing in the same direction as it was in the initial step. The displacement of the top hinge in the direction y can be written as the interval $<h;\ 0>$. The whole course of the mapping is so repeated until the top hinge reaches the last step. This occurs, as soon as the coordinate $y = 0$ and, at the same time, the coordinate $x = L$. In Fig.2, there is presented the displacement of the top hinge. The step of controlled displacement is denoted p.

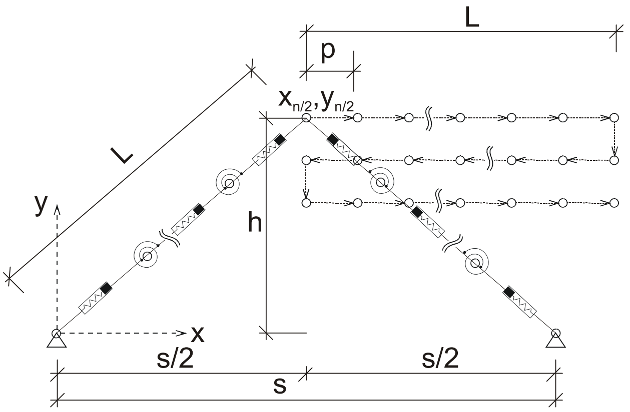

Fig.2 Description of shifting of top hinge

The potential energy of top hinge is recorded in such a way. To be possible to find when the von Mises planar truss is in the stable static eqilibrium state or in the unstable static eqilibrium state, it is suitable to draw the values of transformed potential energy $\overline{U}$ in a clear illustration. The value of transformed potential energy is obtained from the relation of potential energy of the top hinge U to the value of potential energy of the top hinge being on the coordinate x in the half span of the von Mises planar truss $U_{x_{n/2}}$, for the appropriate coordinate y. For any coordinate y, this equation can be written in the following way:

$$\overline{U} = \frac{U}{U_{x_{n/2}}} \tag{7}$$

4 Analysis of von Mises planar trusses

The profile of bars was hot-rolled IPE400, with cross-section area A = 8446 mm^2, second moment of area about minor axis is I = 231.3·10^{-6} m^4, and Young's modulus is E = 210 GPa. The relaxation time t_{rel} = 10 s. Models were generated both with and without initial geometrical imperfection. The initial geometrical imperfection was introduced on the left bar in form of a half wave of the function sinus with a = 0.1 m. The pyramidality changed according to angle α, see Fig.1. The following von Mises planar trusses: α = 45°, α = 55° and α = 60° were studied, on the basis of parameter α. In Fig.3 to Fig.8, there is presented the transformed potential energy (vertical axis) of these models. The transformed potential energy is written within the interval. The grafic presentation was regulated by the condition that, if there occurs the value higher than 1.2 in calculation of transformed potential energy, this value will be set as 1.2. The top hinge displaces in the step p = 0.02 m in coordinate raster $x \in \langle 0;8 \sim 6 \rangle$ and $y \in \langle 0;4 \sim 5 \rangle$.

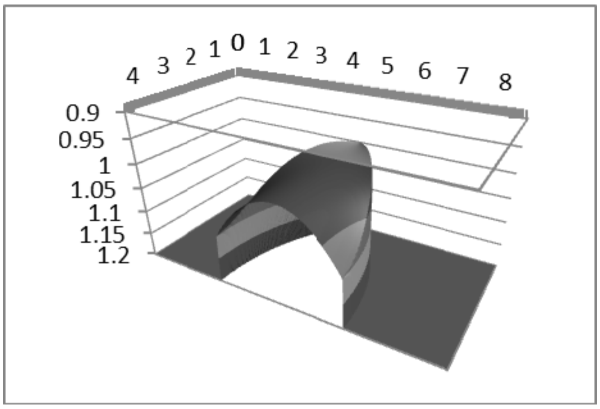

Fig.3 $\overline{U}$ for von Mises truss with α = 45° without imperfection

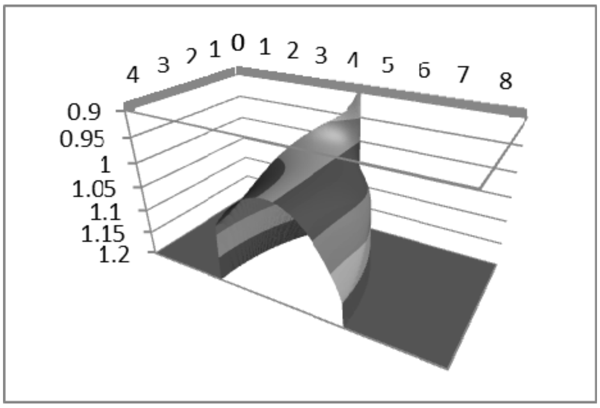

Fig.4 $\overline{U}$ for von Mises truss with α = 45° with imperfection

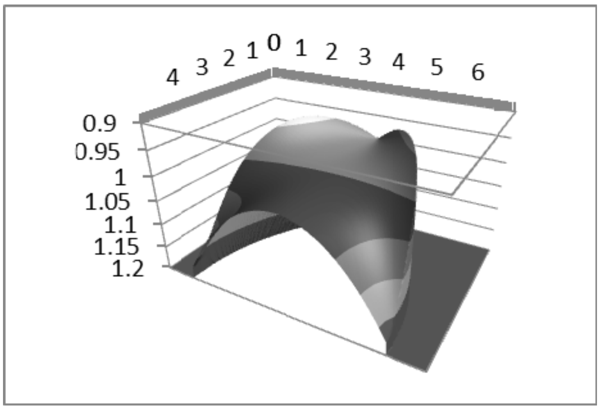

Fig.5 $\overline{U}$ for von Mises truss with α = 55° without imperfection

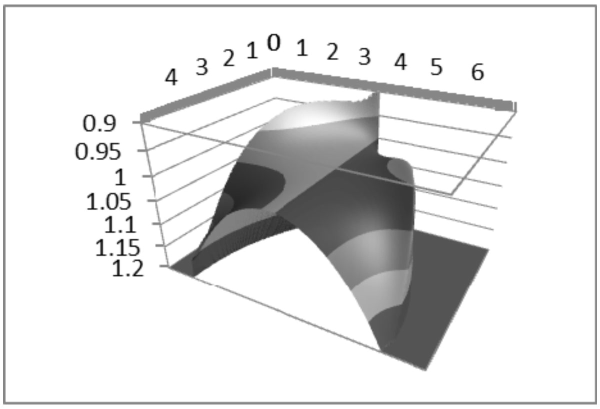

Fig.6 $\overline{U}$ for von Mises truss with α = 55° with imperfection

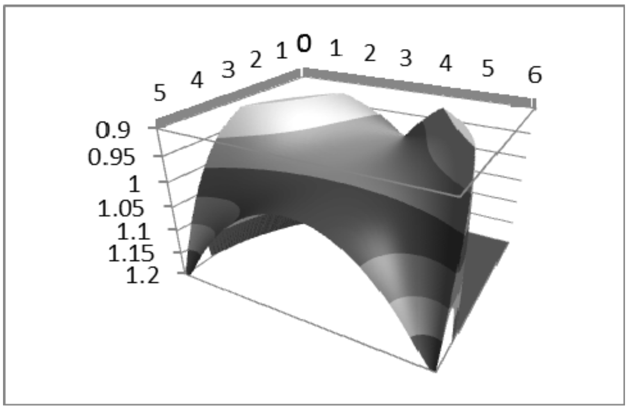

Fig.7 $\overline{U}$ for von Mises truss with α = 60° without imperfection

It can be seen in Fig.3 that the transformed potential energy of top hinge does not decrease at its displacement. The von Mises planar truss is becoming stable. Opposite to it, by introduction of imperfection or by increasing the pyramidality, the transformed potential energy decreases.

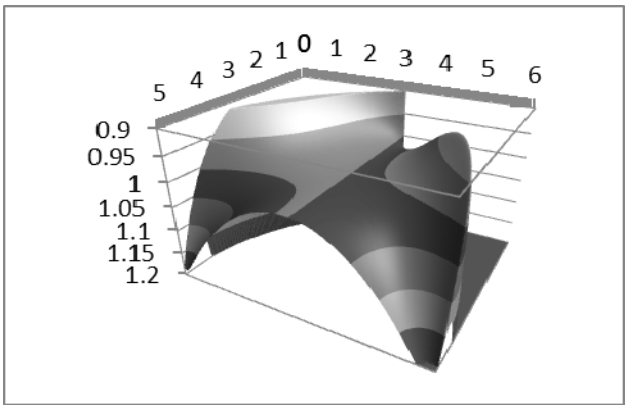

Fig.8 $\overline{U}$ for von Mises truss with α = 60° with imperfection

Thanks to introduction of imperfection into the models, the diagrams of potential energy of the top hinge displacing within the rectangular raster *x*, *y* are not symmetrical, see Fig.8, Fig.6 and Fig.4.

Extremes of transformed potential energies, and/or courses of static eqilibrium paths can be found by a more throughout study. These extremes are divided into minimums of potential energy, stable static eqilibrium state, and maximums of potential energy, and into unstable static eqilibrium state. Bifurcation points can be found in models with imperfections. The points are concerned where the stable static equilibrium state is in contact with the unstable static equilibrium state. Coordinates and values of the transformed potential energy of bifurcation points are given in Table 1.

Angle	Symbol	Coord. X	Coord. Y	$\overline{U}$
45°	B_1	2.98 m	2.39 m	0.9898
55°	B_2	4.07 m	4.11 m	1.011
	B_3	5.37 m	2.13 m	1.0236
	B_4	2.46 m	1.86 m	0.9938
60°	B_5	3.50 m	4.71 m	1.0092
	B_6	2.16 m	1.57 m	0.9975

Table 1 Coordinates and values of transformed potential energies $\overline{U}$ of bifurcation points

5 Conclusion

The present paper studies stability problems by transformed potential energy of pyramidal von Mises planar trusses. The mathematical procedure of the applied method of dynamic relaxation which monitored the transformed potential energy of top hinge was demonstrated. The process of generation of flat and three-dimensional maps of transformed potential energy was presented. The map has shown that, for the von Mises planar truss with lower pyramidality, the transformed potential energy does not decrease. Further on, the maps have shown that introduction of imperfection or increase of pyramidality influences the stability of the von Mises planar truss. Static eqilibrium paths were determined and positions of bifurcation points were identified, based on these facts.

Acknowledgement
The article was elaborated within the framework of project GAČR 14-17997S.

References:

[1] T. V. Galambos, *Guide to Stability design Criteria for Metal Structures*, John Wiley & Sons, 1998, p. 911.
[2] Z. Kala, J. Melcher, L. Puklicky, Material and Geometrical Characteristics of Structural Steels Based on Statistical Analysis of Metallurgical Products, *Journal of Civil Engineering and Management*, Vol.15, No.3, 2009, pp. 299–307.
[3] Z. Kala, Elastic Lateral-torsional Buckling of Simply Supported Hot-rolled Steel I-beams with Random Imperfections, *Procedia Engineering*, Vol.57, 2013, pp. 504-514.
[4] J. Valeš, Effect of Random Axial Curvature on the Performance of Open and Closed Section Steel Columns, *AIP Conference Proceedings*, Vol.1558, 2013, pp. 2512-2515.
[5] Z. Kala, J. Kala, Resistance of Plate Girders Under Combined Bending and Shear, *In Proc. of the 3rd WSEAS Int. Conf. on Engineering Mechanics, Structures, Engineering Geology (EMESEG '10)*, Corfu Island (Greece), 2010, pp. 166-171.
[6] J. Kala, Z. Kala, Large-deflection-theory Analysis of the Effect of Web Initial Curvature on the Ultimate Strength of Steel Plate Girder, *AIP Conference Proceedings*, Vol.1389, 2011, pp. 1861-1864.
[7] Z. Kala, J. Kala, M. Škaloud, B. Teplý, Sensitivity Analysis of the Effect of Initial Imperfections on the (i) Ultimate Load and (ii) Fatigue Behaviour of Steel Plate Girders, *Journal of Civil Engineering and Management*, Vol.11, No.2, 2005, pp. 99-107.
[8] Z. Kala, J. Kala, Resistance of Thin-walled Plate Girders under Combined Bending and Shear, *WSEAS Transactions on Applied and Theoretical Mechanics*, Vol.5, No.4, 2010, pp. 242-251.
[9] A. Omishore, Verification of Design Procedures of Structural Stability using Probabilistic Methods of Reliability Analysis, *AIP Conference Proceedings*, Vol.1479, , No.1, 2012, pp. 2082-2085.
[10] Z. Kala, Reliability Analysis of the Lateral Torsional Buckling Resistance and the Ultimate Limit State of Steel Beams, *Journal of Civil Engineering and Management*, Vol.21, No.7, 2015, pp. 902–911.
[11] Z. Kala, J. Valeš, Modelling and Statistical Approaches to Lateral-torsional Buckling, *Advanced Materials Research*, Vol.969, 2014, pp. 259-264.
[12] J. Valeš, Analysis of Load-carrying Capacity of Thin-walled Closed Beams with Different Slenderness, *Advanced Materials Research*, Vol.969, 2014, pp. 39-40.
[13] Z. Kala, Influence of Partial Safety Factors on Design Reliability of Steel Structures - Probability and Fuzzy Probability Assessments, *Journal of Civil Engineering and Management*, Vol.13, No.4, 2007, pp. 291-296.
[14] Z. Kala, Sensitivity and Reliability Analyses of Lateral-torsional Buckling Resistance of Steel Beams, *Archives of Civil and Mechanical Engineering*, Vol.15, No.4, 2015, pp. 1098-1107.
[15] A. Omishore, Uncertainty Analysis of the Cross-sectional Area of a Structural Member, *In Proc. of the 4th WSEAS Int. Conf. on Engineering Mechanics, Structures*, Engineering Geology (EMESEG '11), Corfu Island (Greece), 2011, pp. 284–288.
[16] A. Omishore, Uncertainty Forecasting in Civil Engineering, Problems and Applications, *In Proc. of the 6th WSEAS Int. Conf. on Applied and Theoretical Mechanics (MECHANICS '10)*, Athens (Greece), 2010, pp. 126–128.
[17] Z. Kala, Sensitivity Analysis of Carrying Capacity of Steel Plane Frames to Imperfections, *AIP Conference Proceedings*, Vol.1048, 2008, pp. 298-301.
[18] Z. Kala, J. Kala, Sensitivity Analysis of Stability Problems of Steel Structures using Shell Finite Elements and Nonlinear Computation Methods, *WSEAS Transactions*

on Applied and Theoretical Mechanics, Vol.4, No.3, 2009, pp. 105-114.

[19] Z. Kala, Sensitivity Analysis in Advanced Building Industry, *Procedia - Social and Behavioral Sciences*, Vol.2, No.6, 2010, pp. 7682-7683.

[20] Z. Kala, J. Kala, Uncertainty and Sensitivity Analysis of Beam Stability Problems using Shell Finite Elements and Nonlinear Computational Approach, *In Proc. of the 11th International Conference on Structural Safety and Reliability, ICOSSAR 2013*, New York, (United States), 2013, pp. 3033-3036.

[21] J. Antucheviciene, Z. Kala, M. Marzouk, E.R. Vaidogas, Solving Civil Engineering Problems by Means of Fuzzy and Stochastic MCDM Methods: Current State and Future Research, *Mathematical Problems in Engineering*, Vol.2015, 2015, Article number 362579.

[22] J. Antucheviciene, Z. Kala, M. Marzouk, E.R. Vaidogas, Decision Making Methods and Applications in Civil Engineering, *Mathematical Problems in Engineering*, Vol.2015, 2015, Article number 160569.

[23] J. Antucheviciene, E. K. Zavadskas, A. Zakarevicius, Ranking Redevelopment Decisions of Derelict Buildings and Analysis of Ranking Results, *Economic Computation and Economic Cybernetics Studies and Research*, Vol. 46, No.2, 2012, pp. 37-62.

[24] F. Fedorik, J. Kala, A. Haapala, M. Malask, Use of design optimization techniques in solving typical structural engineering related design optimization problems, *Structural Engineering and Mechanics*, Vol.55, No.6, 2015, pp. 1121-1137.

[25] J. Kala, P. Hradil, M. Bajer, Reinforced concrete wall under shear load – Experimental and nonlinear simulation, *International Journal of Mechanics*, Vol.9, 2015, pp. 206-212.

[26] J. Atkočiūnas, T. Ulitinas, S. Kalanta, G. Blaževičius, An Extended Shakedown Theory on an Elastic–plastic Spherical Shell, *Engineering Structures*, Vol.101, 2015, pp. 352-363.

[27] S.S. Ligarò, P.S. Valvo, Large Displacement Analysis of Elastic Pyramidal Trusses, *International Journal of Solids and Structures*, Vol.43, No.16, 2006, pp. 206-212. 43, pp. 4867-4887.

[28] M. Kalina, Static Task of von Mises Planar Truss Analyzed using the Potential Energy, *AIP Conference Proceedings*, Vol.1558, 2013, pp. 2107-2110.

[29] R. von Mises, Über die Stabilitätsprobleme der Elastizitätstheorie, ZAMM 3, 1923, pp. 406-422.

[30] R. von Mises, J. Ratzersdorfer, Die Knicksicherheit von Fachwerken, ZAMM 5, 1925, pp. 218-235.

[31] E. Hairer, Ch. Lubich, G. Wanner, Geometric Numerical Integration Illustrated by the Störmer/Verlet method, *Acta Numerica,* Vol.12, 2003, pp.399-450.

[32] P. Frantík, Simulation of the stability loss of the von Mises truss in an unsymmetrical stress state, *Journal Engineering Mechanics*, Vol.14, 2007, pp.155-162.